European Journal of Neuroscience, Vol. 15, pp. 1077–1084, 2002

Superposition of horseshoe-like periodicity and linear tonotopic maps in auditory cortex of the Mongolian gerbil

Holger Schulze, Andreas Hess, Frank W. Ohl and Henning Scheich
Leibniz Institute for Neurobiology, Brenneckestr. 6, 39118 Magdeburg, Germany

Keywords: cocktail-party phenomenon, foreground–background decomposition, Mongolian gerbil, optical recording of intrinsic signals, winner-takes-all algorithm

Abstract

The segregation of an individual sound from a mixture of concurrent sounds, the so-called cocktail-party phenomenon, is a fundamental and largely unexplained capability of the auditory system. Speaker recognition involves grouping of the various spectral (frequency) components of an individual's voice and segregating them from other competing voices. The important parameter for grouping may be the periodicity of sound waves because the spectral components of a given voice have one periodicity, viz. fundamental frequency, as their common denominator. To determine the relationship between the representations of spectral content and periodicity in the primary auditory cortex (AI), we used optical recording of intrinsic signals and electrophysiological mapping in Mongolian gerbils (*Meriones unguiculatus*). We found that periodicity maps as an almost circular gradient superimposed on the linear tonotopic gradient in the low frequency part of AI. This geometry of the periodicity map may imply competitive signal processing in support of the theory of 'winner-takes-all'.

Introduction

The analysis of sound periodicity, whilst yielding results equivalent to spectral analysis in the case of pure tones, becomes an important and independent source of information in the case of spectrally complex periodic signals. This aspect is particularly relevant for the retrieval of such signals from a sound mix. Relevant correlates of periodicity analysis in the auditory system have been identified in terms of 'comodulation masking release' (Hall *et al*., 1984; Klump & Langemann, 1995; Nelken *et al*., 1999), 'modulation detection interference' (Yost *et al*., 1989), and analysis of the fundamental frequency of voiced phonemes as a potential basis for speaker recognition in acoustically rich environments (the 'cocktail party effect' described by Cherry, 1953; von der Malsburg & Schneider, 1986; Yost & Sheft, 1993). Neuronal mechanisms reflecting periodicity are found throughout the auditory system (Hose *et al*., 1987; Schreiner & Langner, 1988; Pantev *et al*., 1989; Jen *et al*., 1993; Heil *et al*., 1995; Langner *et al*., 1997; for review see Langner, 1992) and in primary auditory cortex (AI) neurons respond selectively to both specific tones and periodicities (Schreiner & Urbas, 1988; Eggermont, 1994; Gaese & Ostwald, 1995; Bieser & Müller-Preuss, 1996; Schulze & Langner, 1997, 1999).

This study investigated whether the two aspects of sound, frequency and periodicity, have different spatial representations in AI of the Mongolian gerbil. Because AI is defined by a geometrically precise linear tonotopic gradient (Scheich *et al*., 1993; Thomas *et al*., 1993) it seemed relevant to determine the geometric relationships, i.e. dependence or independence, between the representations of these two parameters superimposed in one cortical area. Therefore, a particular design of amplitude-modulated (AM) tones was used to distinguish between responses to frequency and periodicity. AI was mapped using optical recording of intrinsic signals (ORIS) and microelectrode recording.

Parts of this study have been presented in abstract form (Schulze *et al*., 2000).

Correspondence: Dr Holger Schulze, as above.
E-mail: Holger.Schulze@IfN.Magdeburg.de

Received 31 August 2001, revised 28 January 2002, accepted 1 February 2002

Materials and methods

Preparation

The left auditory cortex of 16 adult male Mongolian gerbils was exposed by craniotomy under deep halothane (Hoechst, Frankfurt a.M., Germany) and local tetracain (Gingicain; Hoechst) anaesthesia leaving the dura intact. A 2.5-cm-long aluminium bar was fixed to the frontal bones with dental acrylic and served as a head anchor for stereotactic fixation. Electrophysiological experiments were performed immediately after preparation, ORIS experiments after one day of recovery. In one animal in which the methods were combined, electrophysiology was carried out immediately after the last ORIS experiment. During the course of experiments anaesthesia was maintained by application (s.c.) of a mixture of ketamine (Ketavet, 50 mg/mL; Pharmacia & Upjohn, Erlangen, Germany), xylazine (Rompun 2%; Bayer, Leverkusen, Germany) and isotonic NaCl solution (mixture 9 : 1 : 10) at a rate of 0.06 mL/h. Body temperature was maintained at 37 °C by a remote-controlled heating pad. For ORIS, a stainless steel recording chamber was cemented over the trepanation area, filled with silicon oil and sealed with a glass coverslip. Animals were examined by extracellular microelectrode recording of single- and multiunit responses ($n = 6$), by ORIS ($n = 9$), or by both methods in combination ($n = 1$).

Handling and care of animals were approved by the ethics committe of the State of Sachsen–Anhalt, Germany.

Auditory stimulation

All recordings were made in an anechoic, sound-attenuated chamber. Stimulation was with pure tones and 100% sinusoidally AM tones, in which the amplitude of the carrier frequency (f_c) was modulated by a modulation frequency (f_m; see Fig. 5, top). Note that the spectrum of AM stimuli consists of the f_c plus two sidebands, $f_c - f_m$ and $f_c + f_m$, where f_m exists only in terms of periodicity of the AM signal and is not a separate spectral component (Fig. 5, middle). For a convincing demonstration of periodicity preference in electrophysiological experiments, f_c had to be high enough to exclude spectral activation of the neurons. Then neurons tuned to low-frequency pure tones that also show tuning to AM tones with low f_m but with f_c above their pure-tone sensitivity are responding only to periodicity in the signal (cf. Schulze & Langner, 1997). All stimuli were presented free-field with 5-ms rise and fall times and 60 ± 5 dB SPL at the animal's ears.

ORIS

Optical records were obtained from the auditory cortex using illumination through two fibre-optic light guides with 605 ± 10 nm band-pass filtered light (DC-regulated tungsten lamp), which gives maximal difference in absorption between oxygenated and deoxygenated haemoglobin (Frostig *et al*., 1990). Acoustic stimuli consisted of either seven pure-tone bursts (0.5, 1, 2, 4, 8, 12 and 16 kHz) or eight AM tones (8 kHz f_c) modulated at 0 (= 8 kHz pure tone), 200, 400, 500, 600, 700, 800 or 1600 Hz (n = 4 animals) or at 200, 283, 400, 566, 800, 1131, 1600 or 2263 Hz (n = 6 animals).

The first set of AM stimuli provides a high-resolution coverage of the octave of periodicities that most units in gerbil AI are tuned to (Schulze & Langner, 1997). The second set of AM stimuli covers the entire range of periodicities in AI with equal spacing (half octave).

In each stimulus presentation eight single consecutive cortical ORIS images (referred to here as 'frames') were collected. Each frame integrated activity over 400 ms. Stimulus onset was triggerd at the beginning frame 2, frame 1 being used to estimate the basic cortical actvity ('reference image' activity R). For each stimulus (500 ms duration) this mode of presentation was repeated four times (repetition rate 1 Hz, starting after the reference image). Different stimuli were presented in a randomized order at regular intervals of 12 s with 50 repetitions. This represents the standard protocol for optical recording of the slow haemodynamic response (Bonhoeffer & Grinvald, 1996). Data from all repetitions were averaged.

Electrophysiology

Responses were recorded extracellularly from single neurons or a small cluster of 2–5 neurons using parylene-coated tungsten microelectrodes (WPI, TM33B10, 1 MΩ; Berlin, Germany) aligned tangentially to the cortical surface (except for the combined-methods animal; see below). Positioning of penetration tracks was measured relative to an anatomical landmark (lambda) to allow topographic reconstruction of recording sites. For the combined methods, electrode penetrations were made radially and penetration sites were marked on an image of the cortical blood-vessel pattern relative to surface vasculature to allow superposition on the ORIS data (Fig. 3D). In all experiments, AM stimuli with an f_c of 8 kHz and f_m ranging from 50 to 3000 Hz were presented randomly at a rate of 2.5 Hz with 200 ms duration. Best periodicities (BPs), i.e. periodicity of the AM tone that elicited the highest discharge rate, were determined from these responses.

Data analysis

In order to obtain baseline-corrected single-condition maps (Bonhoeffer & Grinvald, 1996; Hess & Scheich, 1996), the activity in each frame (F_i, i = 1, …, 7) was corrected for the activity (R) in the reference image by applying $(F_i - R)/R$ for each frame and all repetitions. Very rarely frames occurred containing measuring artefacts; these were excluded from further analysis. To improve signal-to-noise ratio, the image resolution was binned at a bin width of 4 × 4, yielding a resolution of 159 × 141 pixels (pixel size 17 × 17 μm). Images were smoothed by convolution with a 9 × 9 kernel (weighing factor 1). Finally, for each stimulus all frames and all repetitions were averaged, resulting in one image per stimulus. Because the activity (pixel values) in these images is not normally distributed, we subtracted the median value of all pixels within such an image from each single-pixel value. This type of normalization leads to a better comparison of the activity evoked by different stimuli. Maps of best-stimulus representations were computed by determining which stimulus produced the highest activation at each pixel. When the value was < 0, indicating increased oxygen consumption, the pixel was mapped with the colour coding for the best stimulus, otherwise (value $\geqslant 0$) it was coded black. It should be noted that the area activated by a particular stimulus in a single-condition map is larger than the corresponding area in the map of best-stimulus representations, i.e. the area which is activated by the given stimulus more than by any other stimulus in the set. Nevertheless, both types of area measurement correspond with respect to their relative spatial organization in the stimulus map. The latter can be characterized by the spatial pattern of centre of gravity values for each area.

Results

Spatial relation between tonotopic and periodicity ORIS maps

In the ORIS experiments (10 animals), AM stimuli with different f_m (periodicity) but constant f_c activated different coherent areas in AI, which formed a map with an orderly representation of BP (Fig. 1). A circular gradient with a discontinuity (horseshoe-like gradient) of periodicity was revealed by connecting the centres of gravity of the areas representing different frequencies. The maps were located at the dorso-caudal extreme of AI, which is the area where the low-

FIG. 1. Circular topography of periodicity maps in gerbil AI. Panels A–D show horseshoe-like periodicity maps of best stimulus representations from four animals obtained using ORIS with AM stimuli with 8 kHz f_c and different periodicities (f_m, lilac to red codes for increasing periodicity). The maps are superimposed on an image of the cortical surface. Geometry of the topographic organization of these maps was analysed by computing the centres of gravity for each colour patch (white rhombi). White lines connecting the centres of gravity of best-stimulus representations reveal the horseshoe-like gradient of the periodicity map. d, dorsal, c, caudal. Scale bars, 0.5 mm.

FIG. 2. Topography of coincident periodicity and tonotopic maps in gerbil AI. Tonotopic (top panels) and periodicity ORIS maps (bottom panels) are depicted for two animals (A and B), superimposed on an image of the cortical surface. Lilac to red codes for increasing pure-tone frequency f in the top panels, and for increasing periodicity f_m in the bottom panels. Analysis of map geometry as in Fig. 1. Whereas tonotopic maps revealed a linear tonotopic gradient, periodicity maps were characterized by circular gradients of periodicity representation. v, ventral, c, caudal. Scale bars, 0.5 mm.

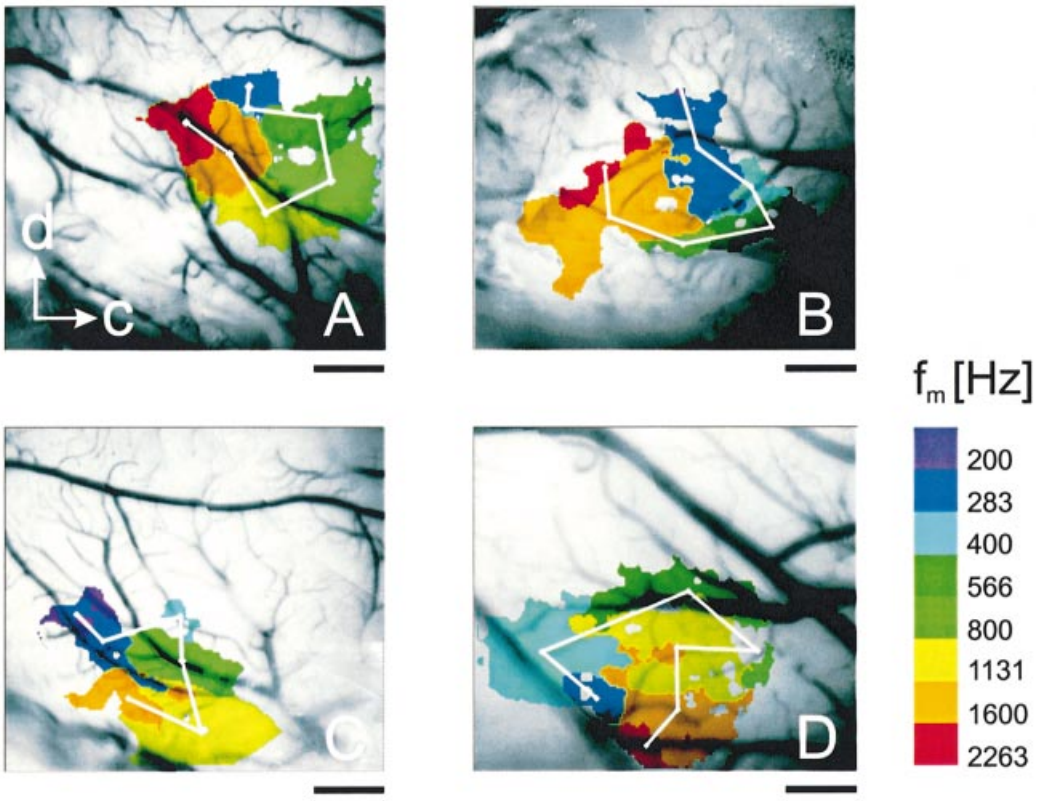
d
c
A
B
C
D
f_m [Hz]
200
283
400
566
800
1131
1600
2263

FIG. 1.

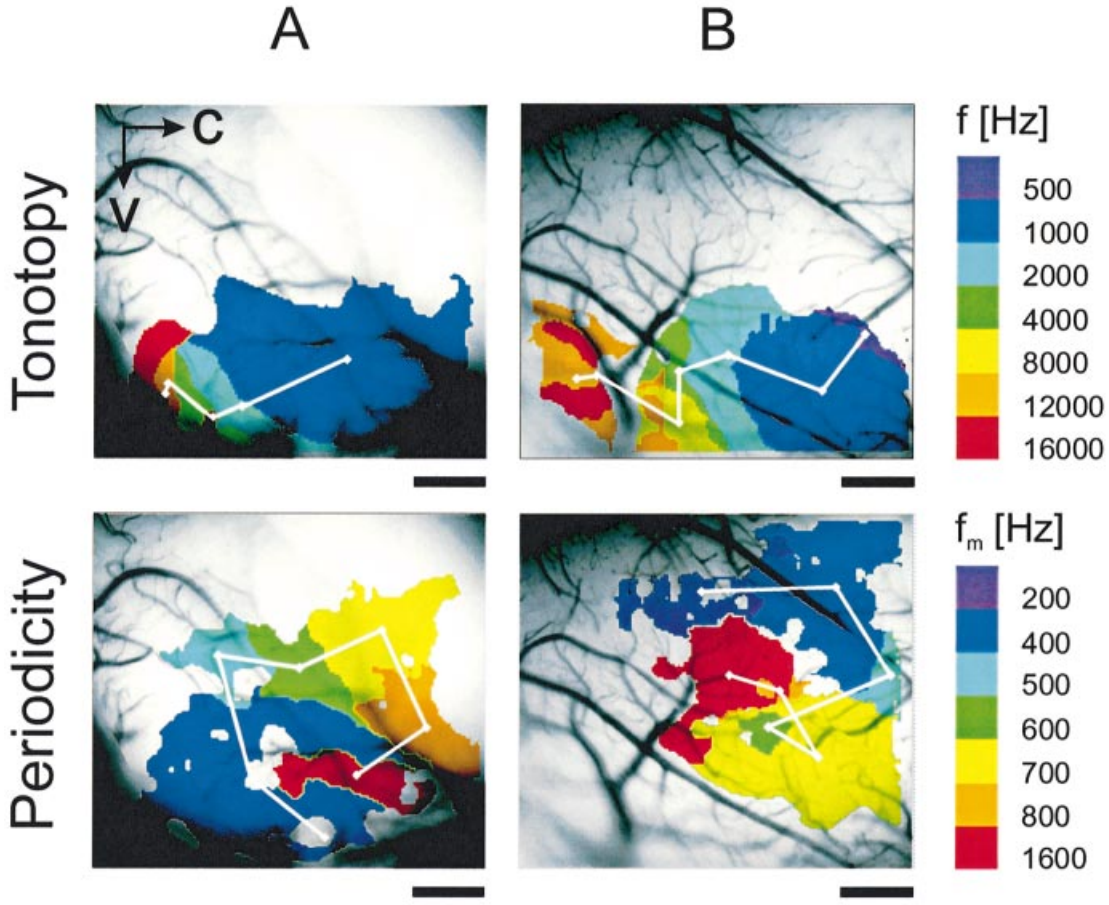
A
B
Tonotopy
c
v
f [Hz]
500
1000
2000
4000
8000
12000
16000
Periodicity
f_m [Hz]
200
400
500
600
700
800
1600

FIG. 2.

frequency range of pure tones is represented in the tonotopic maps obtained with ORIS (Fig. 2). However, the total extent of the two maps differed individually: in six animals the periodicity map extended a few hundred microns more dorsally than the tonotopic map but did not include the rostral, high-frequency area of AI (cf. Fig. 2B); in the other four animals the periodicity map overlapped the high-frequency area, which represents the spectral content of the AM stimuli (cf. Fig. 2A).

The orientation of the periodicity gradient was clockwise in 13 out of 16 animals (cf. Fig. 1) and counter-clockwise in the rest (cf. Fig. 3B–D). The rotation of the periodicity maps relative to the stable rostrocaudal tonotopic gradient varied between individuals. Thus the two maps in the same neural substrate seem to be relatively independent. In some animals, the periodicity map had anomalies in its topographic organization, e.g. the locations of two adjacent BP representations within the gradient were inverted (Fig. 2B, lower panel) or an area of BP formed two separate subareas (e.g. Fig. 3D). Therefore, in contrast to the great interindividual stability of all spatial aspects of the tonotopic map, the only stable aspect of the periodicity map appears to be its circular geometry.

Electrophysiological maps

These results are consistent with electrophysiological mapping of the periodicity of the AM tone that elicited the strongest responses (periodicity tuning) from each neuron (seven animals; Fig. 3A–C). The spatial organization can be determined from these plots by interpolating between the recording positions at which the BP of each neuron was determined. The horseshoe-like circular geometry of the ORIS periodicity map was confirmed by connecting the centres of gravity of areas comprising consecutive octave bands of BP determined electrophysiologically (insets Fig. 3A–C). Because electrophysiology produces a map with coarser spatial resolution than ORIS, other methods of interpolation (cf. Schulze & Langner, 1997) may support a linear gradient model for some maps; however, our method revealed a horseshoe-like organization in all the maps. The clockwise (Fig. 3A) or counter-clockwise (Fig. 3B and C) orientations of the periodicity maps and their varying degrees of rotation provided further confirmation of the ORIS results.

Comparison of methods

Because ORIS and electrophysiological mapping measure different correlates of neuronal activity (see Materials and methods), the question is whether their results can be superimposed in a stencil-like fashion in individuals. Using both methods in one animal (Fig. 3D) it was found that all BPs except one (550 Hz in the light-blue patch) were within half an octave of the f_m identified by ORIS. Outside the region identified in the ORIS experiments, the AM stimuli did not evoke discharges, although these neurons were responsive to pure

TABLE 1. Statistical analysis of geometries of functional gradients

	Linear model ($r = a + bl$)	Quadratic model ($r = a + bl + cl^2$)
Tonotopy data		
	$R^2 = 0.84$	$R^2 = 0.85$
	DF = 42	DF = 42
	$F = 209.81$	$F = 109.23$
	$a = 0.03 \pm 0.03$, $t = 0.93$, $P = 0.360$ (n.s.)	$a = 0.00 \pm 0.04$, $t = 0.0$, $P = 0.99$ (n.s.)
	$b = 0.74 \pm 0.05$, $t = 14.48$, $P = 0.00$	$b = 1.01 \pm 0.19$, $t = 5.4$, $P = 3.0 \times 10^{-6}$
		$c = -0.27 \pm 0.18$, $t = -1.5$, $P = 0.14$ (n.s.)
Periodicity data		
	$R^2 = 0.23$	$R^2 = 0.77$
	DF = 66	DF = 66
	$F = 19.04$	$F = 105.76$
	$a = 0.14 \pm 0.03$, $t = 5.04$, $P = 4.0 \times 10^{-6}$	$a = 0.00 \pm 0.02$, $t = -0.03$, $P = 0.97$ (n.s.)
	$b = 0.19 \pm 0.04$, $t = 4.36$, $P = 4.7 \times 10^{-5}$	$b = 1.24 \pm 0.09$, $t = 13.9$, $P = 0.00$
		$c = -1.05 \pm 0.09$, $t = -12.2$, $P = 0.00$

Analysis of the fits (e.g. Press *et al*., 1988) of the linear model and the quadratic model to both the tonotopy data and the periodicity data. The linear model provides a good fit to the tonotopy data ($R^2 = 0.84$) but not to the periodicity data ($R^2 = 0.23$). The periodicity data require at least a quadratic model for the fit. For further explanations refer to the Results. R^2, coefficient of determination; DF, degrees of freedom; F, F-value from ANOVA; a, b, c, model coefficients; t, t-value of each coefficient; P, attainable significance level for each coefficient.

FIG. 3. Electrophysiological maps of periodicity in AI and their correspondence with ORIS mapping. Panels A–C show locations of responses from extracellular single- and multineuron records (cf. Schulze & Langner, 1997, 1999) from three animals (rhombi). Numbers refer to best periodicities (BP, periodicity of the AM tone that elicited the highest discharge rate). Dashes indicate recording locations where no response was evoked by AM stimuli. Black lines and colours separate octave bands of BPs. Data in panel B are replotted from a previous study (Schulze & Langner, 1997). In panel D combined ORIS and electrophysiological mapping in one animal is shown. Numbers referring to BPs at the recording sites are superimposed on the ORIS map (coloured patches). Insets (top right of each diagram) show the periodicity gradient obtained from centres of gravity for each BP–octave band (coloured dots). Scale bar, 0.5 mm.

FIG. 4. Quantitative analysis of the geometry of the tonotopic and periodicity maps. (A)Schematic drawing of a functional topographic (tonotopic or periodotopic) gradient illustrating the parameters used to analyse geometrical map properties: P_0, P_1, …, P_{n-1} are centres of gravity for best stimulus representations connected by bold lines representing the functional gradient along a contour C; d_1, d_2, …, d_{n-1}, interpoint distances; r_i, Euclidean distances between P_i and P_0 (dotted lines). For a linear geometry (B, blue contour) plotting the values r_i vs. the arc length (see eqn 1) results in a straight graph (C, blue line). For a cyclic geometry (B, red contour) the same analysis results in a curved graph (C, red line). Note that this graph would only curve back to zero if the gradient showed a closed topography. (D)Similar plots for the tonotopic data (blue, dashed lines) and for the periodotopic data (red, dashed lines). Bold lines show the results of the statistical fits of the tonotopic (blue) and periodotopic (red) data to a linear and a quadratic model, respectively. The tonotopy data (dashed blue lines) are well fitted by a linear equation (solid blue line), whereas at least a quadratic equation (solid red line) was needed to fit the periodicity data (dashed red lines). See also Table 1.

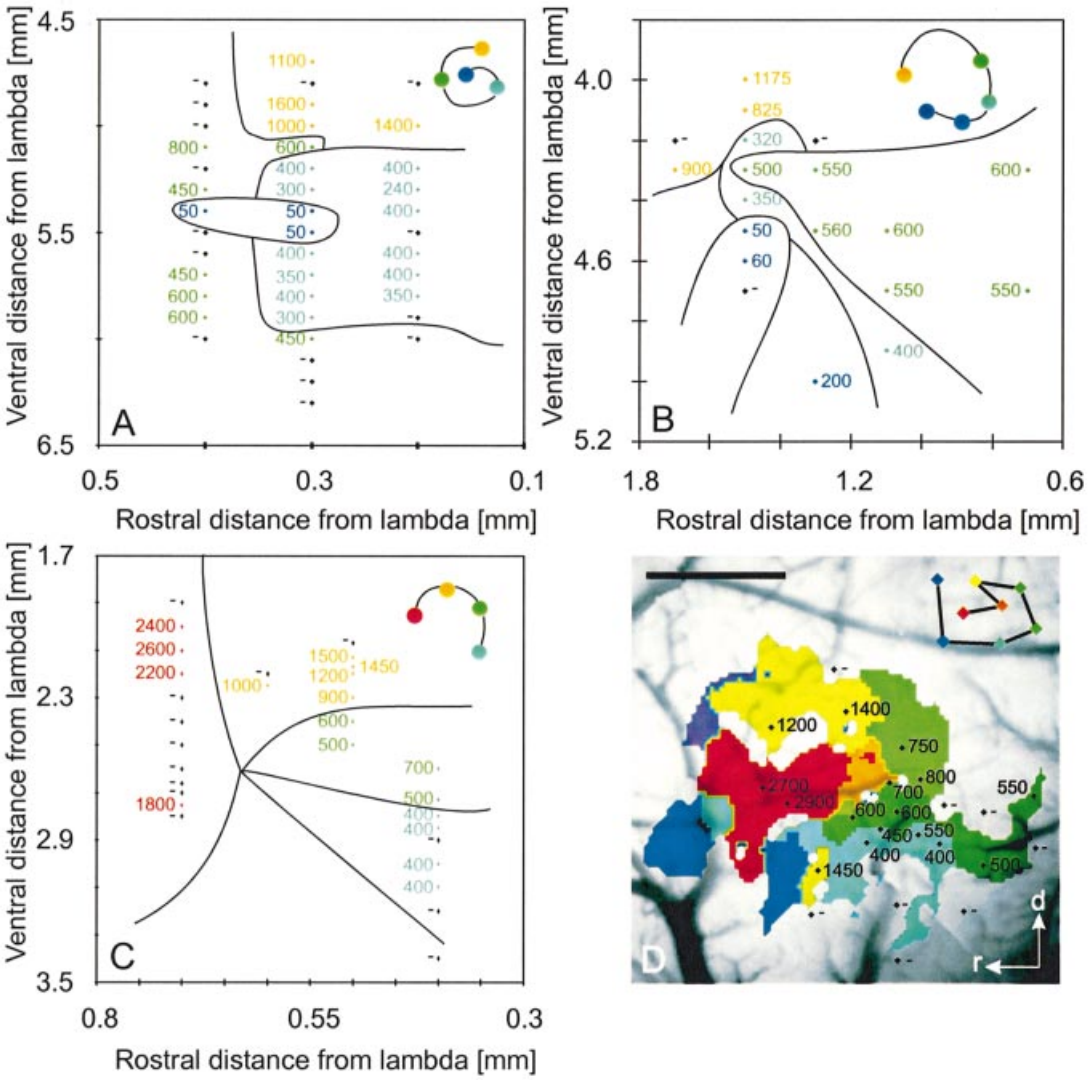
Ventral distance from lambda [mm]
Rostral distance from lambda [mm]
A
B
C
D
4.5
5.5
6.5
0.5
0.3
0.1
4.0
4.6
5.2
1.8
1.2
0.6
1.7
2.3
2.9
3.5
0.8
0.55
0.3
d
r

FIG. 3.

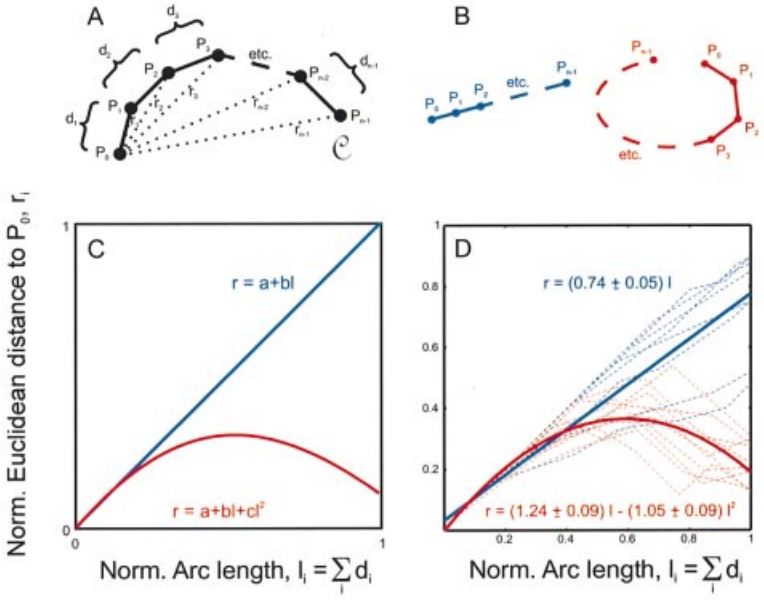
A
B
C
D
etc.
r = a+bl
r = a+bl+cl²
r = (0.74 ± 0.05) l
r = (1.24 ± 0.09) l - (1.05 ± 0.09) l²
Norm. Euclidean distance to P0, ri
Norm. Arc length, li = ∑ di

FIG. 4.

tones (dashes in Fig. 3D). One anomaly in the periodicity map was detected with both methods (extra yellow patch in the ventral part of the map; BP = 1450 Hz).

Quantitative analysis of map geometries

In order to scrutinize the geometric interpretation of the tonotopic and periodotopic maps they were compared to each other by parametric modelling the geometrical properties of the centres of gravity of best stimulus representations. The analysis was as follows.

For each ordered set of n stimuli S_0, S_1, …, S_{n-1} (viz., ascending pure tone frequency in tonotopy experiments or ascending periodicity in periodicity experiments, respectively), the centres of gravity P_0, P_1, …, P_{n-1} for each stimulus representation formed a series of corresponding points with interpoint distances d_1, d_2, …, d_{n-1} along a contour C on the cortical surface (Fig. 4A). For each point P_i along C, the Euclidean distance r_i between P_i and the first point on C (P_0) was plotted vs. the arc length

$$l_i = \sum_{j=1}^{i} d_j \text{ for } i = 1, \ldots, n-1$$

from P_0 to P_i along the contour. Both Euclidean distances r_i and arc lengths l_i were normalized to the total length of C. If stimuli S_0, S_1, …, S_{n-1} were mapped along a straight contour (Fig. 4B, blue) this plot should result in the linear function $r = l$ (Fig. 4C, blue). For any curved contour, this plot should indicate smaller distance values r_i for corresponding arc lengths than those that lie on the linear function $r = l$. In particular, if the curvature is such that C curves back into the geometrical neighbourhood of P_0 (Fig. 4B, red), the Euclidean distances r_i should converge to values near zero as the normalized arc length l_i approaches the value 1.0 (Fig. 4C, red). The data pairs (l_i,r_i) obtained in tonotopy as well as periodicity experiments were fitted to both a linear (affine) function $r(l) = a + bl$ and a quadratic function $r(l) = a + bl + cl^2$. Parameters a, b and c were chosen to minimize the residual sum of squares between data and model. Experiments were compared on the basis of the fitted parameters a, b and c and the goodness of the fits.

The results of this analysis are shown in Fig. 4D in which plots of Euclidean distances r_i vs. arc lengths l_i are illustrated for both the tonotopy (blue) and periodicity (red) experiments. Measured data are shown by dashed curves; the linear fit for the tonotopy data (blue) and the quadratic fit for the periodicity data (red) are shown as continuous curves. Table 1 summarizes the results of the statistical analysis of both fits to both tonotopy data and periodicity data. For each fit, the values given are the coefficient of determination R^2, which provides a first means to estimate the goodness of fit, the F-value and the degrees of freedom of a statistical comparison (ANOVA) of the model with a model involving only a constant term, as well as estimators of the model's coefficients (a, b, c), together with their corresponding t-value and attainable significance levels (e.g. Press *et al.*, 1988). It is obvious from this analysis that the linear model provides a good fit to the tonotopy data (coefficient of determination $R^2 = 0.84$) but not to the periodicity data ($R^2 = 0.23$). The inadequacy of the linear model for the periodicity data can also be inferred from a statistical comparison (ANOVA) of the linear model with a model involving only a constant term. This comparison yielded an F-value ($F_{66} = 19.04$) much smaller than the degrees of freedom (66), a result which is indicative of the inadequacy of the linear model for the periodicity data. Also, the meaningful result of a constant term close to zero was only yielded by the linear model and not by the quadratic model. The

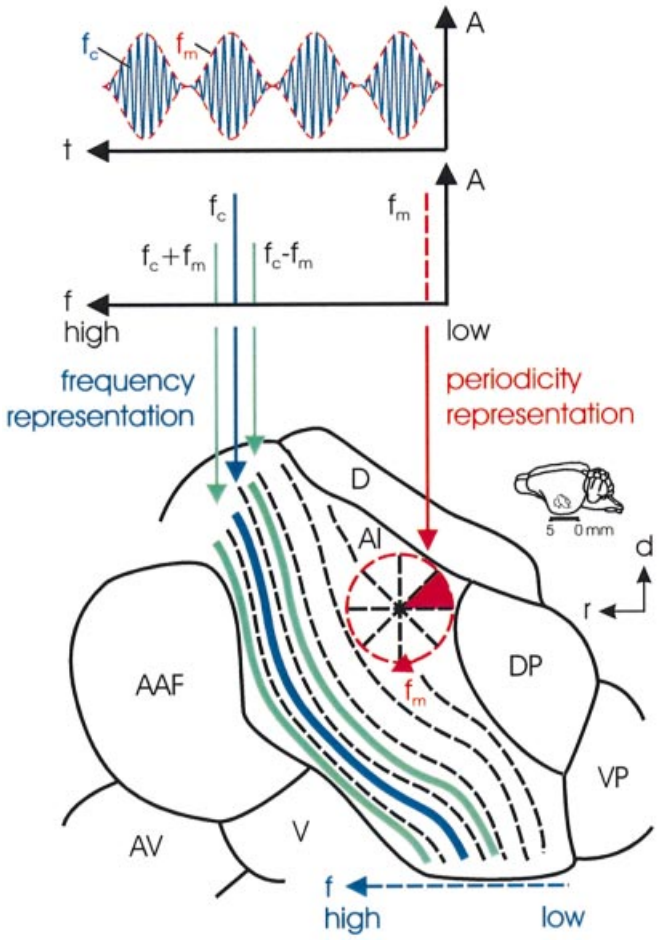

FIG. 5. Scheme of spectral and temporal representations of AM tones in the gerbil AI. Top, waveform (amplitude over time) and spectrum (amplitude over frequency) of an AM signal. The modulation frequency f_m, corresponding to the envelope of the waveform (dashed red line), is not found in the spectrum. Below, diagram of the auditory fields in gerbil cortex (adapted from Thomas *et al.*, 1993) with a schematic drawing of the circular periodicity map superimposed on the linear tonotopic map illustrating the topographic representation in AI of an AM stimulus used in our study (high f_c, low f_m). Note that the periodicity map is bigger than sketched in this figure (cf. Figs 1 and 2). The spectrum of the stimulus is represented rostrally as isofrequency contours in the high-frequency part of the tonotopic map (blue bands), whereas the periodicity of the stimulus (red sector) is represented in the periodicity map, which is centred in the dorsocaudal low-frequency region. The geometry of the linear tonotopic gradient is denoted by the blue dashed arrow and the horseshoe-like, circular periodicity gradient by red dashed arrow. AAF, anterior auditory field; AV, V, D, DP, and VP, secondary auditory fields; d, dorsal; r, rostral.

periodicity data were successfully fitted by the quadratic model as indicated by the variance analytic comparison with a constant term model ($F_{66} = 105.76$). The model was able to reproduce the vanishing constant term a and yielded estimates for b and c, significantly different from zero. As the tonotopy data could be fitted already by the linear model, the quadratic model consequently was also appropriate to fit these data ($F_{42} = 109.23$), but with the quadratic factor c not significantly different from zero. Hence, this analysis demonstrated the appropriateness of the linear model for the tonotopic organization and the requirement of at least a quadratic model for the periodotopic organization of the maps in AI. Whilst the first result is in agreement with earlier data (Thomas *et al.*, 1993;

Hess & Scheich, 1996) the latter result revealed a circular, horseshoe-like topography of the periodicity map which was previously not revealed.

Discussion

In this report we describe the superposition of the representations of two important parameters of sound, frequency and periodicity, in the primary auditory cortex of the gerbil (cf. Fig. 5). Although AM with only one f_c was used to describe the circular map, it is likely that periodicity is indeed the stimulus parameter represented. Earlier electrophysiological studies (Schulze & Langner, 1997, 1999) showed that changes of BPs by variation of f_c are only small and nonsystematic. Specifically, it was found that across units the BP could increase or decrease with increasing f_c, and that the direction of BP change varied nonsystematically among closely neighbouring units. In extrapolation of these data no qualitative changes to the overall map organization as revealed by the ORIS technique are expected.

The circular geometry of the periodicity map is unexpected because the parameter represented is not cyclic. The functional explanation for such a map may lie in the geometry of the topographic stimulus representation which, it is generally postulated, affects the neuronal computations that can be carried out within a map (Nelson & Bower, 1990; Scheich, 1991; Goodhill & Sejnowski, 1997). If so, our results indicate that the optimal algorithms required to process periodicity information differ from those optimal for spectral analysis. Given suitable connectivity between neurons, a horseshoe-like, circular arrangement of best-stimulus representations could facilitate several types of interaction that are not possible in a linear map. For example, the proximity of best-stimulus representations across the centre of the map would allow neurons representing a certain value of a stimulus, such as periodicity, to make equivalent interconnections with neurons representing all other values of that parameter. Such a pattern of interconnections could facilitate computational algorithms for which synchronous interactions between arbitrary distances in the parameter space are critical (see below).

On the basis of these considerations we put forward the hypothesis that one possible functional interpretation of the circular geometry of the described periodicity map may be that such a map geometry could provide a pattern of interconnections that facilitates the extraction of a particular value of the represented parameter from a mixture of other values by a neuronal implementation of a 'winner-takes-all' algorithm (Haken, 1991; Schmutz & Banzhaf, 1992; Waugh & Westervelt, 1993). This would be in addition to the lateral interaction mechanism thought to operate in linear topographic maps, where only the contrast between neighbouring neurons (and stimulus representations) is enhanced. In this sense, the map of amplitudes composed of two facing half-cycles of amplitude representation in the auditory cortex of the mustached bat (Suga, 1977) and the pinwheel-like arrangement of the iso-orientation domains in the visual cortex (Bonhoeffer & Grinvald, 1991) may also be substrates for a winner-takes-all computation, a hypothesis that to our knowledge has not been tested.

The identification of individual signals from a mixture is a common task for the auditory systems of all vocalizing species (Bodnar & Bass, 1999). Gerbils are social animals living as family groups in elaborate burrows, with many such groups in the vicinity (Thiessen & Yahr, 1977; Ågren *et al*., 1989). They have a rich repertoire of vocalizations, including a group of alarm calls one of which is characterized by harmonic spectra with periodicities in the range represented in the map reported here (Yapa, 1994). There, harmonics are in a narrow band (20–26 kHz) with a periodicity around 2 kHz, very similar to the AM stimuli we used in our study.

A 'winner-takes-all' algorithm operating in a circular, horseshoe-like periodicity map as suggested above that extracts a stimulus with one particular periodicity out of a mixture of stimuli with different periodicities might therefore already be useful for the gerbil to distinguish between different individuals vocalizing within a group. Analogously, the same mechanism might be used by humans to extract the periodicity (fundamental) of a speaker's voice out of a mixture of different speakers (cocktail-party effect; Cherry, 1953; von der Malsburg & Schneider, 1986; Yost & Sheft, 1993). Whether a secondary area in human auditory cortex which was shown to be involved in foreground–background decomposition (Scheich *et al*., 1998) uses a similar map for extracting the periodicity (fundamental) of a specific speaker's voice in noisy situations remains to be seen.

Acknowledgements

This study was supported by the Deutsche Forschungsgemeinschaft, Schwerpunktprogramm 'Zeitgebundene Informationsverarbeitung im zentralen auditorischen System'. We are grateful to Dr Birgit Gaschler-Markefski for support in the statistical analysis and to Dr Jennifer Altman for editorial help with the manuscript.

Abbreviations

AI, primary auditory cortex; AM, amplitude modulated; BP, best periodicity; f_c, carrier frequency; f_m, modulation frequency; ORIS, optical recording of intrinsic signals; R^2, coefficient of determination.

References

Ågren, G., Zhou, Q. & Zhong, W. (1989) Ecology and social behaviour of Mongolian gerbils, *Meriones unguiculatus*, at Xilinhot, Inner Mongolia, China. *Anim. Behav.*, **37**, 11–27.

Bieser, A. & Müller-Preuss, P. (1996) Auditory responsive cortex in the squirrel monkey: neural responses to amplitude modulated sounds. *Exp. Brain. Res.*, **108**, 273–284.

Bodnar, D.A. & Bass, A.H. (1999) Midbrain combinatorial code for temporal and spectral information in concurrent acoustic signals. *J. Neurophysiol.*, **81**, 552–563.

Bonhoeffer, T. & Grinvald, A. (1991) Iso-orientation domains in cat visual cortex are arranged in pinwheel-like patterns. *Nature*, **353**, 429–431.

Bonhoeffer, T. & Grinvald, A. (1996) Optical images based on intrinsic signals. In Toga, A.W. & Mazziotta, J.C. (eds), *Brain Mapping: the Methods*. Academic Press, London, pp. 55–97.

Cherry, E.C. (1953) Some experiments on the recognition of speech, with one and with two ears. *J. Acoust. Soc. Am.*, **25**, 975–979.

Eggermont, J.J. (1994) Temporal modulation transfer functions for AM and FM stimuli in cat auditory cortex. Effects of carrier type, modulating waveform and intensity. *Hear. Res.*, **74**, 51–66.

Frostig, R.D., Lieke, E.E., Ts'o, D.Y. & Grinvald, A. (1990) Cortical functional architecture and local coupling between neuronal activity and the microcirculation revealed by in vivo high-resolution optical imaging of intrinsic signals. *Proc. Natl Acad. Sci. USA*, **87**, 6082–6086.

Gaese, B.H. & Ostwald, J. (1995) Temporal coding of amplitude and frequency modulation in the rat auditory cortex. *Eur. J. Neurosci.*, **7**, 438–450.

Goodhill, G.J. & Sejnowski, T.J. (1997) Objective functions for the topography: a comparison of optimal maps. In Bullinaria, J.A., Glasspool, D.G. & Houghton, G. (eds), *Proceedings of the Fourth Neural Computation and Psychology Workshop: Connectionist Representations*. Springer, London.

Haken, H. (1991). *Synergetic Computers and Cognition*. Springer, Berlin.

Hall, J.W., Haggard, M.P. & Fernandes, M.A. (1984) Detection in noise by spectro-temporal pattern analysis. *J. Acoust. Soc. Am.*, **76**, 50–56.

Heil, P., Schulze, H. & Langner, G. (1995) Ontogenetic development of periodicity coding in the inferior colliculus of the Mongolian gerbil. *Aud. Neurosci.*, **1**, 363–383.

Hess, A. & Scheich, H. (1996) Optical and FDG mapping of frequency-specific activity in auditory cortex. *Neuroreport*, **7**, 2643–2647.

Hose, B., Langner, G. & Scheich, H. (1987) Topographic representation of periodicities in the forebrain of the Mynah bird: One map for pitch and rhythm? *Brain. Res.*, **422**, 367–373.

Jen, P.H.-S., Hou, T. & Wu, M. (1993) Neurons in the inferior colliculus, auditory cortex and pontine nuclei of the FM bat, *Eptesicus fucus* respond to pulse repetition rate differently. *Brain Res.*, **613**, 152–155.

Klump, G.M. & Langemann, U. (1995) Comodulation masking release in a songbird. *Hear. Res.*, **87**, 157–164.

Langner, G. (1992) Periodicity coding in the auditory system. *Hear. Res.*, **60**, 115–142.

Langner, G., Sams, M., Heil, P. & Schulze, H. (1997) Frequency and periodicity are represented in orthogonal maps in the human auditory cortex: evidence from magnetoencephalography. *J. Comp. Physiol. A*, **181**, 665–676.

von der Malsburg, C. & Schneider, W. (1986) A neural cocktail-party processor. *Biol. Cybern.*, **54**, 29–40.

Nelken, I., Rotman, Y. & Yosef, O.B. (1999) Responses of auditory-cortex neurons to structural features of natural sounds. *Nature*, **397**, 154–157.

Nelson, M.E. & Bower, J.M. (1990) Brain maps and parallel computers. *Trends Neurosci.*, **13**, 403–408.

Pantev, C., Hoke, B., Lütkenhöner, B. & Lehnhertz, K. (1989) Tonotopic organization of the auditory cortex: pitch versus frequency representation. *Science*, **246**, 486–488.

Press, W.H., Flannery, B.P., Teukolsky, S.A. & Vetterling, W.T. (1988). *Numerical Recipes in C.* Cambridge University Press, Cambridge.

Scheich, H. (1991) Auditory cortex: comparative aspects of maps and plasticity. *Curr. Opin. Neurobiol.*, **1**, 236–247.

Scheich, H., Baumgart, F., Gaschler-Markefski, B., Tegeler, C., Tempelmann, C., Heinze, H.J., Schindler, F. & Stiller, D. (1998) Functional magnetic resonance imaging of a human auditory cortex area involved in foreground-background decomposition. *Eur. J. Neurosci.*, **10**, 803–809.

Scheich, H., Heil, P. & Langner, G. (1993) Functional organisation of auditory cortex in the Mongolian gerbil (*Meriones unguiculatus*): II. Tonotopic 2-deoxyglucose. *Eur. J. Neurosci.*, **5**, 898–914.

Schmutz, M. & Banzhaf, W. (1992) Robust competitive networks. *Phys. Rev. A*, **45**, 4132–4145.

Schreiner, C.E. & Langner, G. (1988) Periodicity coding in the inferior colliculus of the cat. II. Topographical organization. *J. Neurophysiol.*, **60**, 1823–1840.

Schreiner, C.E. & Urbas, J.V. (1988) Representation of amplitude modulation in the auditory cortex of the cat. II. Comparison between cortical fields. *Hear. Res.*, **32**, 49–64.

Schulze, H., Hess, A., Ohl, F.W. & Scheich, H. (2000) Optical imaging reveals cyclic periodotopic map in gerbil auditory cortex. *Association for Research in Otolaryngology, Abstracts of the 23rd Midwinter Research Meeting*, Vol. 23, 20–24 February 2000, St Petersburg, FL, USA. Association for Research in Otolaryngology, Mt Royal, NJ, USA, p. 16.

Schulze, H. & Langner, G. (1997) Periodicity coding in the primary auditory cortex of the Mongolian gerbil (*Meriones unguiculatus*): Two different coding strategies for pitch and rhythm? *J. Comp. Physiol. A*, **181**, 651–663.

Schulze, H. & Langner, G. (1999) Auditory cortical responses to amplitude modulations with spectra above frequency receptive fields: evidence for wide spectral integration. *J. Comp. Physiol. A*, **185**, 493–508.

Suga, N. (1977) Amplitude spectrum representation in the Doppler-shifted-CF processing area of the auditory cortex of the mustached bat. *Science*, **196**, 64–67.

Thiessen, D. & Yahr, P. (1977). *The Gerbil in Behavioral Investigations; Mechanisms of Territoriality and Olfactory Communication*. University of Texas Press, Austin, USA.

Thomas, H., Tillein, J., Heil, P. & Scheich, H. (1993) Functional organisation of auditory cortex in the Mongolian gerbil (*Meriones unguiculatus*): I. Electrophysiological mapping of frequency representation and distinction of fields. *Eur. J. Neurosci.*, **5**, 882–897.

Waugh, F.R. & Westervelt, R.M. (1993) Analog neural networks with local competition. I. Dynamics and stability. *Phys. Rev. E*, **47**, 4524–4536.

Yapa, W.B. (1994) Social behaviour of the Mongolian gerbil Meriones unguiculatus, with special reference to acoustic communication. Dissertation, *University of Munich*.

Yost, W.A. & Sheft, S. (1993) Auditory perception. In Yost, W.A., Popper, A.N. & Fay, R.R. (eds), *Human Psychophysics*. Springer, New York, pp. 193–236.

Yost, W.A., Sheft, S. & Opie, J. (1989) Modulation interference in detection and discrimination of amplitude modulation. *J. Acoust. Soc. Am.*, **86**, 2138–2147.